Cooling rate dependence of structural properties of aluminium during rapid solidification

2001 J. Phys.: Condens. Matter 13 1873

(http://iopscience.iop.org/0953-8984/13/9/311)

INSTITUTE OF PHYSICS PUBLISHING JOURNAL OF PHYSICS: CONDENSED MATTER

J. Phys.: Condens. Matter **13** (2001) 1873–1890 www.iop.org/Journals/cm PII: S0953-8984(01)19706-7

Cooling rate dependence of structural properties of aluminium during rapid solidification

C S Liu, Z G Zhu, Junchao Xia and D Y Sun

Laboratory of Internal Friction and Defects in Solids, Institute of Solid State Physics, Chinese Academy of Sciences, PO Box 1129, Hefei 230031, People's Republic of China

Received 1 December 2000, in final form 15 January 2001

Abstract

Constant-pressure molecular dynamics simulations and a systematic analysis of the local atomic structures have been performed to study the structural evolution of aluminium on different cooling runs. The regular and defective icosahedral atomic configurations depend strongly on the cooling rate, which is responsible for the cooling rate dependence of the enthalpy. In the simulated amorphous aluminium there exist three kinds of microstructure unit that do not depend on the cooling rate. Two of them are similar to those in the fcc crystal containing interstitialcy and hardly change with decreasing temperature after the glass formation. The third can be considered as crystal germs. Our results also suggest that there exists a critical cooling rate below which the icosahedra form a percolating cluster and the glass exhibits high stability. At a certain quenching rate that is slower than this critical cooling rate, the strength of the icosahedron clusters infinite network may have a saturation value, i.e. a maximum. This may be the origin of the existence of an ideal quenching rate at which the glass exhibits the highest structural stability.

1. Introduction

As well known, in the process of solidification the cooling rate plays a very important role. If a material is quenched fast enough, the end product will be an amorphous solid, i.e. a glass; if cooled slowly the end product will be a crystalline solid. There is a critical cooling rate separating glass forming and crystal forming. Much attention has been paid to the dependence of some macroscopic and microscopic quantities on the cooling rate in glass systems. In experiments [1, 2] and in computer simulation [3], the dependence of some macroscopic quantities such as the density of the glass or the glass transition temperature on the cooling rate has been found. However, from the viewpoint of microstructures, the exact reason for this dependence is not clear. Recently, in computer simulations [4–6], it has been shown that certain microscopic quantities depend on the cooling rate more strongly than the macroscopic quantities do. For example, using the Lennard-Jones potential, Vollmayr and co-workers [4] have investigated the dependence of bulk properties of a glass on the cooling rate. By studying the clusters formed by the nearest-neighbour shell of the central atom, they have shown that

0953-8984/01/091873+18$30.00

a variation of the cooling rate over four decades leads to a change in enthalpy of only 1–2% but a change in probability of finding a cluster of type $A_{12,1}$ by as much as 20% (where $A_{12,1}$ means that the central atom, being of type A, has 12 nearest neighbours with one of them being of type B). It is the cooling rate dependence of the distribution function for the clusters rather than the individual properties of the clusters themselves that will give rise to the cooling rate dependence of the enthalpy and the density. Therefore, in order to understand the cooling rate dependence of macroscopic quantities, detailed knowledge of the microstructure and the characterization of the short-range order are essential.

On a model of soft-sphere glass, Jund *et al* [7] have studied the local structure as a function of the quenching rate and the relaxation time. By studying the fraction of pentagonal faces and standard deviation of the Voronoi cell-volume distribution as a function of the quenching rate or the relaxation time, they have shown that the glass quenched faster shows a more pronounced tendency towards crystallization as time goes by, and for a given glass there exists an ideal quenching rate at which the structural stability of the glass is strongest. However as they pointed out in the paper, their explanation did not take into account the ability of the existent crystal germs to grow and the microscopic origin of the existence of such an ideal quenching rate remains to be elucidated.

In the preceding computer simulation studies, a pair potential has usually been used. One of the appealing features of this potential is that it contains only two-body terms, thus avoiding the three-body terms and making it very attractive for computer simulations. Despite the limitation of relatively short times, computer simulations are still likely to be useful in helping us understand the structural properties of glasses, because their use is based on reasonable and justifiable assumption about the fundamental interatomic interactions in a material. In recent years, considerable efforts have been devoted to the study of empirical and semi-empirical many-body potentials for pure metals and binary alloys [8–11], which are easily used in computer calculations. Using many-body potentials, molecular dynamics simulations have been performed to study the glass transition and crystallization during rapid solidification from liquid metals [12, 13], but the cooling rate dependence of the macroscopic and the microscopic properties in glass is seldom studied.

In the present work, by using a many-body potential, the pair analysis techniques and the bond orientational ordering method, we investigate how the quenching rate affects the macroscopic and microscopic properties of aluminium (Al) glass, in hope of gaining an understanding of the characteristics of the glass structure and its behaviour. Some information on the microscopic origin of an ideal quenching rate is obtained. The rest of the paper is organized as follows: in section 2, we sketch out the main computational methods used in the calculations. In section 3, we present and discuss the obtained results. Finally in section 4 we briefly summarize our results.

2. Computational methods

The recently developed *glue* potential [11] can correctly reproduce many basic properties of Al in crystalline and noncrystalline phases. Using this potential, Sun and Gong have successfully studied the structural properties and glass transition in Al clusters [14]. They have obtained that the atomic structures for Al_{13}, Al_{55} and Al_{147} atoms clusters are in agreement with the results from *ab initio* calculations, and demonstrated that the disordered cluster Al_{43} can be considered as a glass cluster. In our present work, the *glue* potential is employed to model the Al atomic interaction. The computer simulation is based on constant-pressure MD simulations [15]. The simulated system consists of 500 atoms in a cubic cell with periodic boundary conditions. The Newtonian equations of motion are integrated using the velocity-Verlet algorithm with a time

step $\Delta t = 5.3 \times 10^{-16}$ s. Firstly, the system is heated up to 1400 K. In the heating process, the enthalpy increases with temperature, and the solid-to-liquid phase transition occurs at about 1125 K, which is in agreement with the critical superheating temperature reported by Lu and Li [16]. Then, the system is run for 50 000 time steps to guarantee an equilibrium liquid state. Finally a rapid quenching starts from the liquid phase. The cooling rates investigated are 1.9×10^{15} ($\gamma 6$), 1.9×10^{14} ($\gamma 5$), 1.9×10^{13} ($\gamma 4$), 9.5×10^{12} ($\gamma 3$), 4.7×10^{12} ($\gamma 2$) and 1.9×10^{12} ($\gamma 1$) K s^{-1}. During every quenching process, the structural configuration is saved at certain time-step intervals. The selected intervals are inverse proportional to the cooling rates, which is expected to lead to the same temperatures of sample points from each cooling process. But because we used the (N, P, H) ensemble, the temperatures of sample points differ a little with cooling rates. For each of the recorded configurations, another run of 12 000 time steps at the given temperature is performed in order to collect data for analysing the macroscopic and microscopic quantities. During each of these runs, 20 configurations are saved and analysed by another program. The results of microstructural analysis indicate that the system does not undergo monotonic change during the sampling processes at a certain temperature. In addition, another simulation from different initial configurations for three cooling processes ($\gamma 6$, $\gamma 5$ and $\gamma 4$) and the use of 4000-atom instead of 500-atom simulations for two faster cooling processes ($\gamma 6$ and $\gamma 5$) were found to have little effect on the calculated results (the cooling dependence of the macroscopic and microscopic quantities) presented below.

The microscopic local structure can be described using the pair analysis technique [17]. In this technique, pairs of atoms are characterized with four indices. The first index indicates whether the pair of atoms is closer than a given cutoff distance. Two atoms are said to be near neighbours or, equivalently, are considered to form a bond (a root pair) if they are within this cutoff distance. The first index is 1 if the pair is bonded and 2 otherwise; these are denoted as type I and II pairs. The second index represents the number of near neighbours shared by the root pair. The third index represents the number of the bonds among the shared neighbours. The fourth index is introduced to resolve the ambiguity about the arrangement of the bonds. In the present work, the position of the first minimum of the pair distribution function is used as the cutoff distance. This method is able to distinguish between various local structures. The relative number of different types of pair is normalized so that the total number of type I pairs is unity. Some typical atomic bond pairs of type I are shown in figure 1. The 1551 pairs (as shown in figure 1(a)), which correspond to two neighbouring atoms with five common neighbours forming a pentagon of near-neighbour contacts, are characteristic of icosahedral ordering, whereas the 1421 pairs (as shown in figure 1(b)) and the 1422 pairs (as shown in figure 1(c)) are characteristic of fcc and hcp crystalline structures respectively. In this figure, we also show the 1541 pairs and 1431 pairs in the fcc Al structure containing linearlike extended split or dumbbell interstitialcy in equilibrium configuration (as shown in figures 1(d) and (e) respectively), and in the Al glass (as shown in figures 1(f) and (g) respectively).

The bond orientational order parameters W_l [18, 19] are also calculated to measure the local orientational symmetry. W_l are sensitive measures of the different orientational symmetries enumerated by Frank. For an icosahedral symmetry, it is sufficient to calculate the orientational order parameter W_6, which is most sensitive to the icosahedral symmetry. W_6 is defined as

$$W_6 = W_6' \Big/ \left[\sum_{m=-6}^{6} |\bar{Q}_{6m}|^2 \right]^{3/2}$$

where

$$W_6' = \sum_{\substack{m_1,m_2,m_3 \\ m_1+m_2+m_3=0}} \begin{bmatrix} 6 & 6 & 6 \\ m_1 & m_2 & m_3 \end{bmatrix} Q_{6m} Q_{6m} Q_{6m}.$$

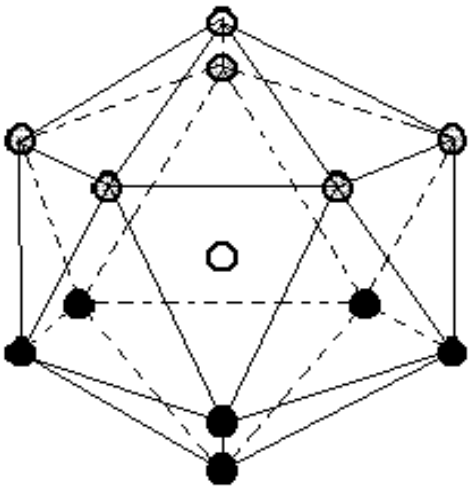

(a)

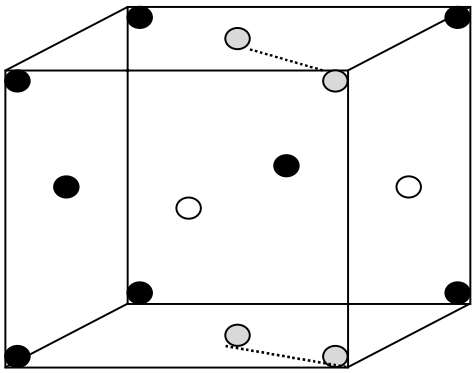

(b)

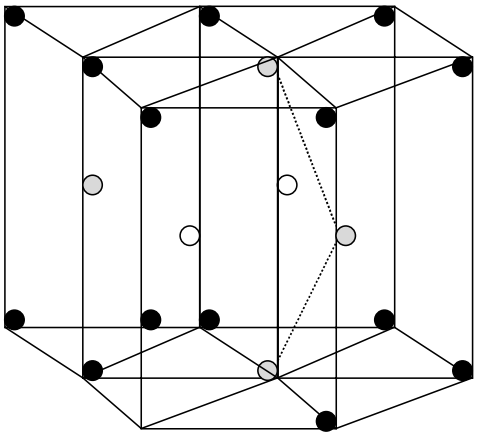

(c)

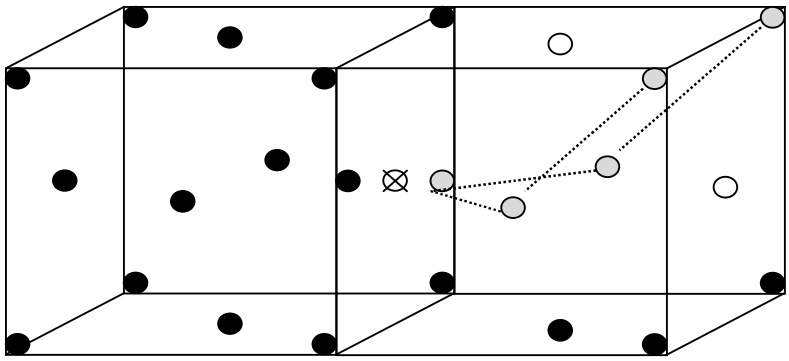

(d)

Figure 1. Schematic diagram of typical pairs, where the root pairs are denoted by open circles, and the common nearest neighbours of the root pairs are denoted by grey circles, (a) the 1551 pair, (b) the 1421 pair, (c) the 1422 pair, (d) the 1541 pair in the interstitialcy model, (e) the 1431 pair in the interstitialcy model, (f) the 1541 pair in the glass, (g) the 1431 pair in the glass.

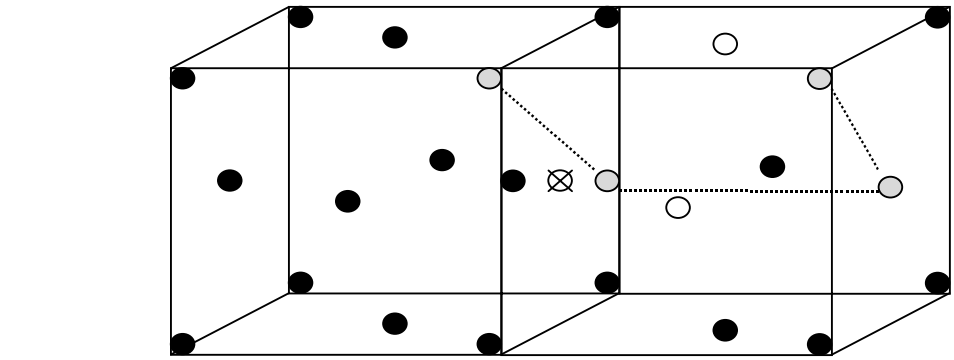

(e)

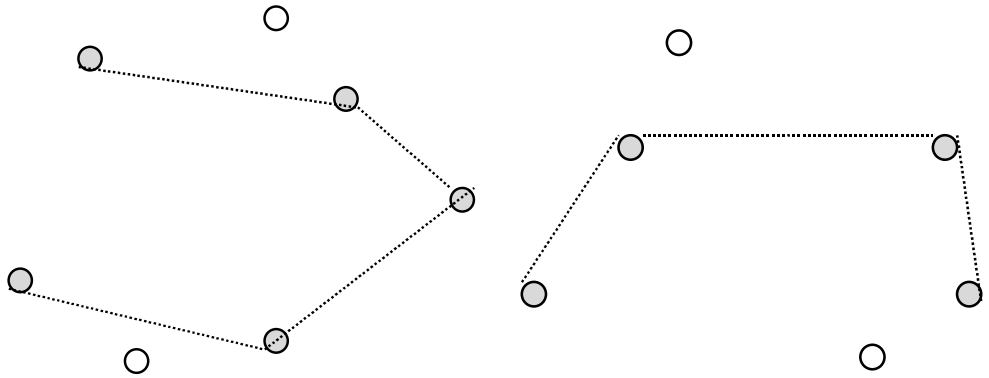

(f) (g)

Figure 1. (Continued)

$Q_{6m} = Y_{6m}(\theta(r), \phi(r))$, $m = -6, \ldots, 0, \ldots, 6$; here Y_{6m} are the spherical harmonics, and $\theta(r)$ and $\phi(r)$ are the polar angles of the bond measured with respect to some reference coordinate system. $\bar{Q_{rm}}(r) = \langle Q_{6m}(r) \rangle$; here the average is taken over some suitable set of bonds in the sample. The coefficients

$$\begin{bmatrix} 6 & 6 & 6 \\ m_1 & m_2 & m_3 \end{bmatrix}$$

are Wigner $3j$ symbols. In the 13-atom icosahedron, W_6 is equal to $-1.697\,54$.

3. Results and discussions

3.1. The changes in some macroscopic properties on cooling runs

Two of the simplest quantities one can study in a cooling process are the enthalpy and the density of the system. Earlier simulations of glass-forming systems by Abraham [20] have shown that the slopes of the enthalpy and the density–temperature curves change sharply or have a bend over a narrow temperature range during a cooling process, while the value of the enthalpy and the density does not abruptly change. It is assumed that, at the temperature where the slope of these curves changes sharply, the system falls out of equilibrium, because the typical relaxation times of the system exceed the time scale of the cooling process. Therefore, this temperature

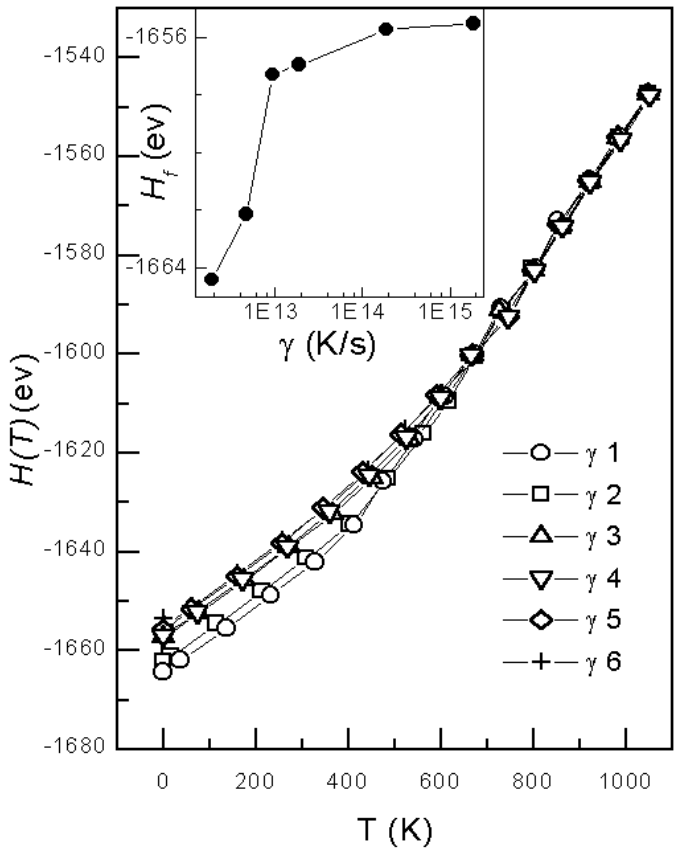

Figure 2. Enthalpy of the system as a function of temperature. Inset: final enthalpy H_f against cooling rate γ.

can be identified with the glass transition temperature T_g. That is, the enthalpy and the density change linearly with decreasing temperature above T_g, whereas below T_g their decrease is still linear but slower. According to Abraham's suggestion, the T_g is the intersection of two lines with different slopes.

The enthalpy of the system, $H(T)$, as a function of temperature for all cooling rates investigated is shown in figure 2 (the density $\rho(T)$ is not presented here since it is similar to the enthalpy). In the high-temperature region, for different cooling rates the curves of $H(T)$ change linearly and are close to each other, emphasizing that the atoms are mobile enough to adapt easily to the speed with which the temperature is changed. In the intermediate temperature region, for all cooling rates these curves have a noticeable bend, and as the cooling rate decreases this bend region moves towards the low temperature. Thus, in this region the intrinsic relaxation times of the atoms become comparable to the available time, which is determined by the cooling rate; the system then falls out of equilibrium. At low temperatures, there is a small but observable dependence of $H(T)$ on the cooling rate in that the larger the cooling rate is the higher the enthalpy is. From a formal point of view, the cooling process can be seen as an optimization problem in which the system tries to minimize the free enthalpy. It will manage to do this better if the more time is given to search for this minimum. These results are similar to that obtained by using the pair potential [21] and, for a cooling rate the changing

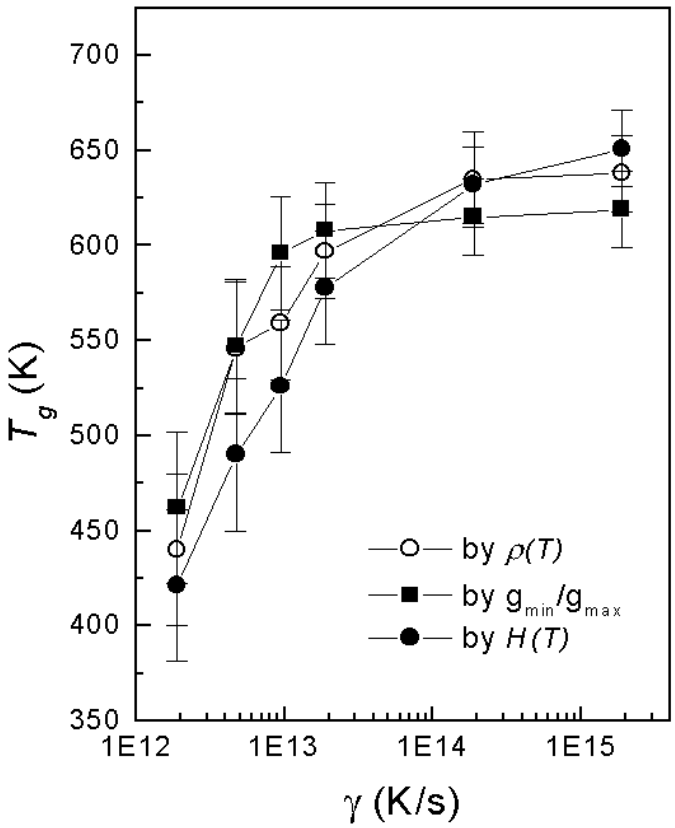

Figure 3. Glass transition temperature T_g as a function of cooling rate γ.

trend of $H(T)$ with temperature is also similar to that obtained by using the embedded-atom potential [12]. From this figure, we see that for very large cooling rates this dependence of $H(T)$ on the cooling rate becomes much weaker; a similar result is also obtained by Vollmayr *et al* [4].

Following Abraham's suggestion [20], we have obtained the glass transition temperature T_g. In figure 3 we show the thus-determined T_g as a function of the cooling rate γ; T_g is obtained from the cooling rate dependence of the enthalpy and the density and an empirical parameter $R(= g_{min}/g_{max}$, where g_{max} and g_{min} are the magnitudes of the first shell maximum and the first minimum following this maximum in the pair distribution function, respectively). We see that a variation of the cooling rate about three decades gives rise to a variation of T_g of about 200 K and the extrapolated T_g derived from different physical quantities are consistent with each other within numerical uncertainties. In the experiments [2]; two kinds of relationship between T_g and $\ln\gamma$ have been obtained: one is a linear dependence of T_g on $\ln\gamma$, the other is well fitted by the function $T_g(\gamma) = T_c^0 + A/\ln(B\gamma)$, where T_c, A and B are fitting parameters. In the recent studies on cooling rate dependence in Lennard-Jones glass [5] and amorphous silica [6], the dependence of T_g on γ is fitted well by the function $T_g(\gamma) = T_0 - B/\ln(A\gamma)$ or $T_g(\gamma) = T_c + (A\gamma)^{1/\delta}$. From figure 3, we also see that the relationship between T_g and $\ln\gamma$ is not similar to the above-mentioned relationship in experiments and simulations. This difference may arise from the following reasons. First, in our present work we studied a pure metal system, in which the interaction between atoms includes many-body terms. Second, the

relationship between T_g and $\ln\gamma$ found in the experiment or simulation largely depends on the range of studied cooling rates [22]. The linear relationship between T_g and $\ln\gamma$ should only be found if one confines oneself to a small range of cooling rates. The larger this range becomes, the more the actual relationship should deviate from linearity. This deviation may be different between the high cooling rates and the low cooling rates. Third, the glass transition temperature is obtained from a fitting procedure whose validity and range of applicability cannot be determined on a sound theoretical basis [22].

We now turn our attention back to the final enthalpy H_f at $T = 0$ K, whose dependence on the cooling rate is shown in the inset in figure 2. A variation of γ of about three decades leads to a change in the enthalpy of only 0.7%. The relationship between H_f and γ also cannot be well fitted by a logarithmic or a power-law function used in some work [5, 6]. On this point, the explanation is the same as that for the glass transition temperature.

3.2. The changes in the microscopic structures on cooling runs

In the previous section, we investigated how the cooling rate influences some macroscopic quantities. The goal of the present section is to see how the cooling rate affects the microscopic quantities of the system and strive to get some information about the macroscopic behaviour.

As the system approaches the glass transition, icosahedral structure clusters increase significantly and the geometrical shapes of such characteristic clusters of atoms must be responsible for the origin of the splitting of the second peak of the pair distribution function [23]. The microscopic quantities firstly investigated are the relative number of 1551 bond pairs, the relative number of regular icosahedra and their bond orientational ordering parameter w_6. Figure 4 presents the relative number of the 1551 bond pairs (we denote it as *HA1551* in the figure) as a function of temperature on all cooling runs. For all quenching processes, the relative number of 1551 bonded pairs increases with decreasing temperature. This changing trend of the 1551 pairs with temperature is in agreement with that in [12], [13] and [21]. From this figure, we can also see that the slower is the cooling rate the larger is the relative number of 1551 pairs, and the cooling rate effect on the 1551 pairs is similar to that on the enthalpy and the density, but the magnitude of this effect is significantly larger than any change we observed for macroscopic quantities, showing that the microscopic properties depend on the cooling rate more strongly than the macroscopic properties do. The relative number of icosahedra and the icosahedral bond orientational order parameters W_6 are given in figures 5(a) and (b). A icosahedron is a polyhedron, whose central atom has 12 neighbouring atoms joined to the central atom by twelve 1551 pairs [24]. From this figure, it is clear that with decreasing temperature, the icosahedral number and the icosahedral orientational order exhibit different behaviour. The changing trend of the former is similar to that of the 1551 pairs and the enthalpy or the density, whereas the latter changes linearly in the whole range of temperature and does not depend on the cooling rate. Therefore, with decreasing temperature both the number of the icosahedra and their orientational ordering increase, whereas with decreasing the cooling rate only the number of the icosahedra increases. A similar relationship between the number of icosahedra and the temperature or the cooling rate is obtained by Kondo and Tsumuraya [25].

In the range of low temperatures, the relative number of 1551 pairs is about 30%, while the relative number of icosahedra is about 4%. So we should investigate the defective icosahedra (a polyhedron consisting of some 1551, 1661, and/or 1441 pairs is called a defective icosahedron [24]). The relative number of defective icosahedra and their orientational ordering W_6 given in figures 6(a) and (b) show a similar behaviour as 1551 pairs. The decrease in the cooling rate gives rise to an increase in the number of defective icosahedra and a decrease in the deviation of the defective icosahedron from the standard icosahedron.

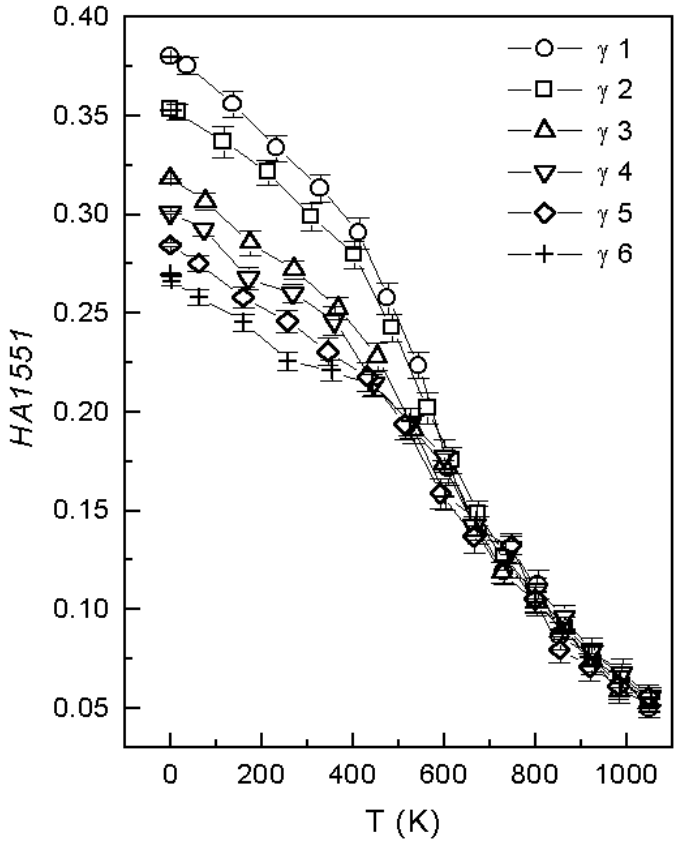

Figure 4. Relationship between relative number of 1551 pairs (*HA1551*) and temperature.

Since 1541 and 1431 pairs represent the short-range ordering in liquid and amorphous states [12, 13, 23], we then investigate these two kinds of bond pair. Figure 7 gives the relative number of 1541 and 1431 pairs as a function of temperature in the cooling processes. At high temperatures, there is a linear increase in two types of pairs, the 1541 and 1431 pairs, whereas at the glass transition temperature these pairs arrive their maxima and, a further decrease of temperature does not lead to any significant change in the 1541 and 1431 pairs. The sum of the relative number of these two kinds of pair is up to 40% after the system has passed the glass transition. From this figure, we can also see that there is an important and interesting phenomenon concerning the relative number of 1541 and 1431 pairs, that is, the relative number of these two pairs is nearly independent of cooling rate, which is completely different from the case of the 1551 pairs and the 1422 pairs (see below). In some papers [12, 13, 23] by the pair analysis technique, the results have shown that the 1541 and 1431 pairs are present in some non-crystalline states and represent the short-range ordering in liquid and amorphous states, but because only one cooling rate is used, the relationships between these two kinds of pair and the cooling rate are absent. For one cooling rate, our present results are in agreement with those in [12], [13] and [23]. Further discussions about these two kinds of pair will be made in the following section.

Now we investigate the 1421 and 1422 bond pairs, which are the characteristics of fcc and hcp crystalline structures respectively. Figures 8(a) and (b) give the changing trend of

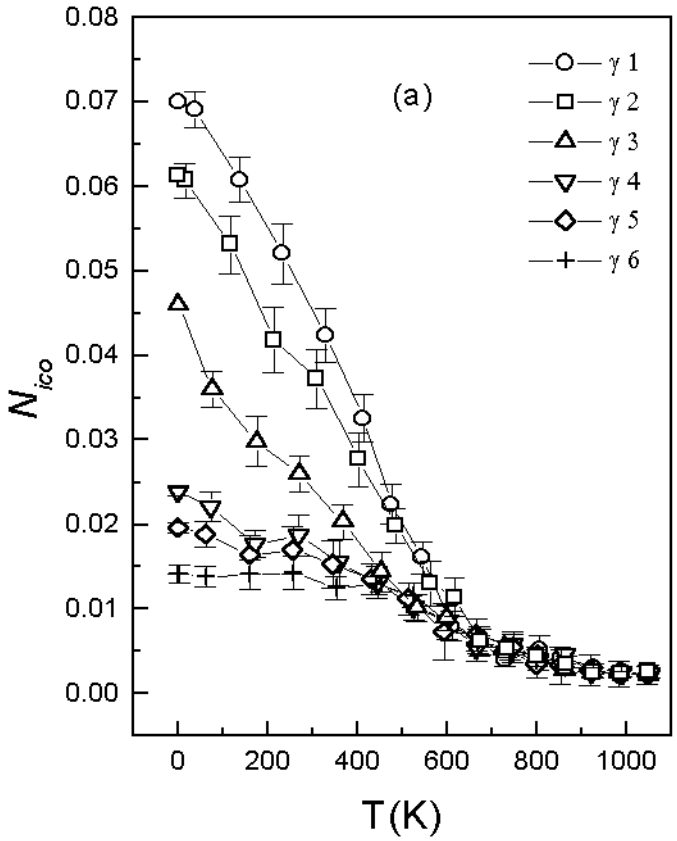

Figure 5. Relative number of icosahedra (N_{ico}) and icosahedral order parameters W_6 against temperature in (a) and (b) respectively.

1421 and 1422 bonded pairs during all cooling processes. The relative number of these two kinds of bond pair increases firstly and then decreases with decreasing temperature. We also find a clear anticorrelation between the crystal pairs (1421 + 1422) and the icosahedral pairs in low-temperature configurations obtained in all cooling process, which may result from crystal nucleation and icosahedral ordering as two competing tendencies. This is in agreement with the results reported by Jonsson and Andersen [21]. From this figure, we can also see that the change in the 1421 pairs is nearly independent of the cooling rate, whereas the relative number of the 1422 pairs decreases with decreasing cooling rate in the range of low temperatures. This may come from the fact that the crystal structure is fcc.

To form a sharp contrast between macroscopic and microscopic quantities, in table 1 we give the magnitude of the changes (Mc) in the enthalpy and some microscopic quantities at zero temperature due to a three-decade variation of the cooling rate from the fastest to the slowest cooling. In table 1 P_a stands for the average probability to find the bond pairs or clusters in the system on six different runs. The signs + and − mean increase and decrease. From this table, the three-decade variation of the cooling rate leads to much stronger changes in some microscopic quantities than the enthalpy, such as the numbers of icosahedra and defective icosahedra and the relative number of the 1551 and 1422 pairs. Combining the magnitude of the changes in the microscopic quantities and their average probability found in the system,

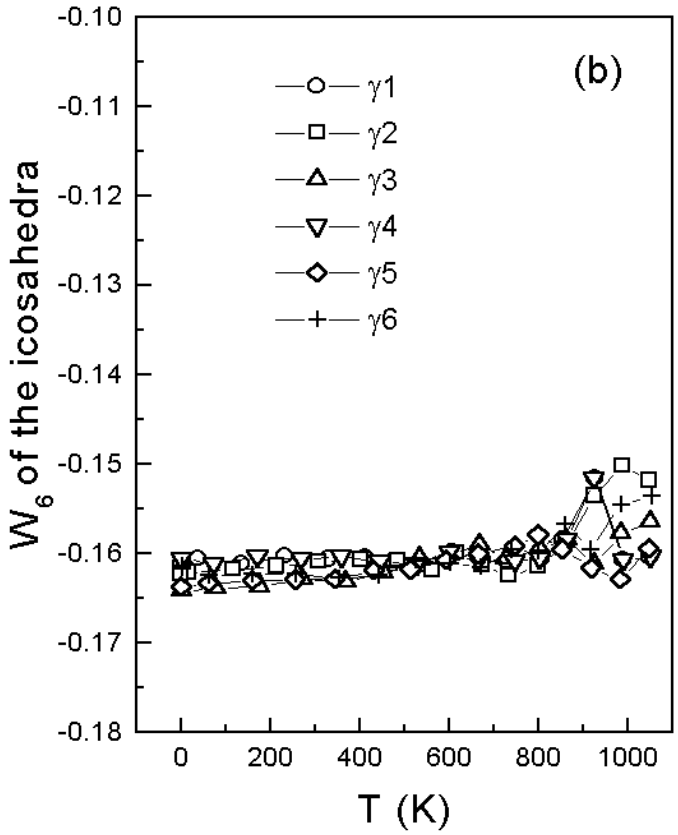

Figure 5. (Continued)

Table 1. The magnitude of the changes (Mc) in the final enthalpy H_f and some microscopic quantities at zero temperature due to a three-decade variation of the cooling rate γ from the fastest to the slowest cooling, and the average probability P_a of finding some bond pairs or clusters in the system for six cooling rates. + and − mean increase and decrease.

	$\gamma_1/\gamma 6$	H_f	$HA1551$	N_{ico}	N_{dico}	$HA1541$	$HA1431$	$HA1421$	$HA1422$
Mc	10^{-3}	−0.7%	+43%	+412%	+40%	−5%	−3%	−6%	−48%
P_a			0.32	0.04	0.08	0.16	0.25	0.05	0.08

we think there are two factors resulting in a change, but much smaller in the enthalpy. One is that with decreasing cooling rate the 1551 pairs increase, that is, the icosahedral ordering increases. Another is that the 1541, 1431 and 1421 pairs do not apparently depend on the cooling rate (also see figures 4 and 5), and the sum of these three kinds of pair is up to 46%.

3.3. Further discussions about some microscopic structures

In the preceding section, we have seen that the 1541 and 1431 pairs arrive at their maxima at the glass transition temperature and a further decrease of temperature does not lead to any significant change in the 1541 and 1431 pairs. The relative numbers of 1541 and 1431 pairs hardly depend of the cooling rate, which is completely different from the case of the 1551

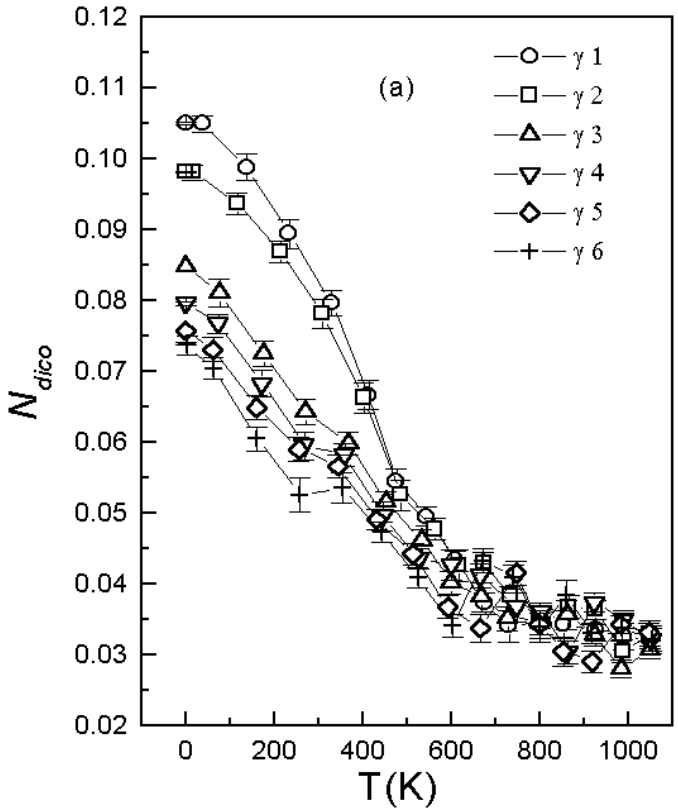

Figure 6. Relative number of defective icosahedra (N_{dico}) and defective icosahedral order parameter W_6 against temperature in (a) and (b) respectively.

pairs and the 1422 pairs. To our knowledge, in contrast with 1551, 1421 and 1422 pairs, the physical picture of these two kinds of pair so far is still limited. Thus, a question arises: what is the reason for the near temperature independence and cooling rate independence of these two kinds of pair after the system has passed the glass transition temperature? The basis of addressing this question is the interstitialcy model suggested recently by Granato [26] for condensed states of fcc metals. Nordlund and Averback [27] have obtained the high interstitial concentration and the maximum allowable superheating, which are in good agreement with the interstitialcy model. In this model, the thermodynamic properties are obtained regarding liquids as crystals containing a few per cent of interstitialcy in thermal equilibrium, while amorphous materials correspond to a fixed concentration c_0 of frozen-in interstitialcy and the concentration c_0 depends on the method of preparation of the material. We know that the equilibrium configuration for an isolated interstitial in Al is not a point defect with cubic symmetry as a vacancy, but rather a linearlike extended dumbbell interstitialcy configuration with tetragonal symmetry. In an fcc metal, an interstitialcy will produce 32 pairs of 1541, 16 pairs of 1431, 16 pairs of 1311, four pairs of 1441 and two pairs of 1401, annihilate 56 pairs of 1421, and finally have an increment of 14 pairs in total bond pairs. The 1441, 1401 and 1311 pairs are not concerned in our present work since their magnitude is small or they can be obtained by a vacancy. From figures 1(d)–(g), we see that the 1541 pairs and the 1431 pairs in Al glasses are very similar to those in the interstitialcy model. The 1541 pairs are not regarded as fivefold symmetric, but the deviation of 1541 pairs from 1551 pairs is much

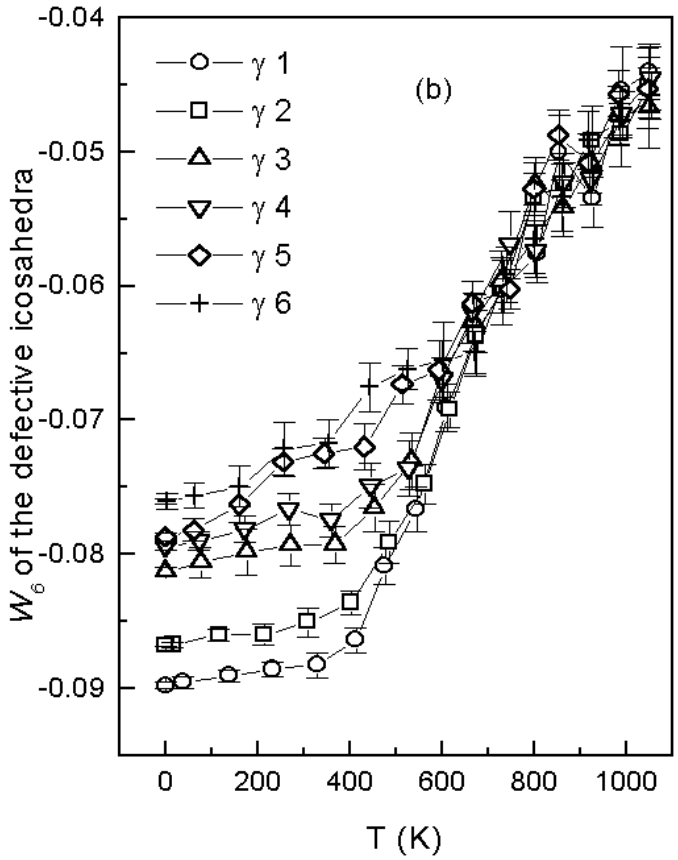

Figure 6. (Continued)

smaller than other kinds of pair. According to the interstitialcy model, after the glass transition the 1541 and 1431 pairs nearly keep constant. Our present result is in agreement with this. In the range of low temperatures, the ratio of the 1541 pairs to the 1431 pairs is about 0.65, which is much smaller than that in the interstitialcy model of fcc metals. However two notes should be pointed out: one is that the ratio of the sum of the 1541 and 1551 pairs to the 1431 pairs is approximately equal to that of the 1541 pairs to the 1431 pairs in the interstitialcy model, implicating that the 1551 pairs may come from the 1541 pairs. Another is that this direct comparison may be very rough. These results also show that in the range of low temperatures the constant number of 1541 and 1431 pairs is a dynamic result, that is, some bonded pairs transform into the 1541 and 1431 pairs and these two kinds of pair transform into other bonded pairs. Based on our results and the interstitialcy model, the concentration c_0 of frozen-in interstitialcy in amorphous states may not depend on the cooling rate. This may be reasonable, since the cooling rates used in our present work are very high. Though the 1541 and 1431 pairs do not depend on the cooling rate, they may play an important role on the dependence of other kinds of pairs on the cooling rate. The role of the 1541 and 1431 pairs is like a bridge which links two different kinds of bonded pair showing different dependences on the cooling rate, for example, the 1551 pairs and the 1422 pairs: the former increase with decreasing cooling rate, whereas the latter decrease. Our obtained results for the 1541 and 1431 pair may be a test on the interstitialcy model for condensed states of fcc metals.

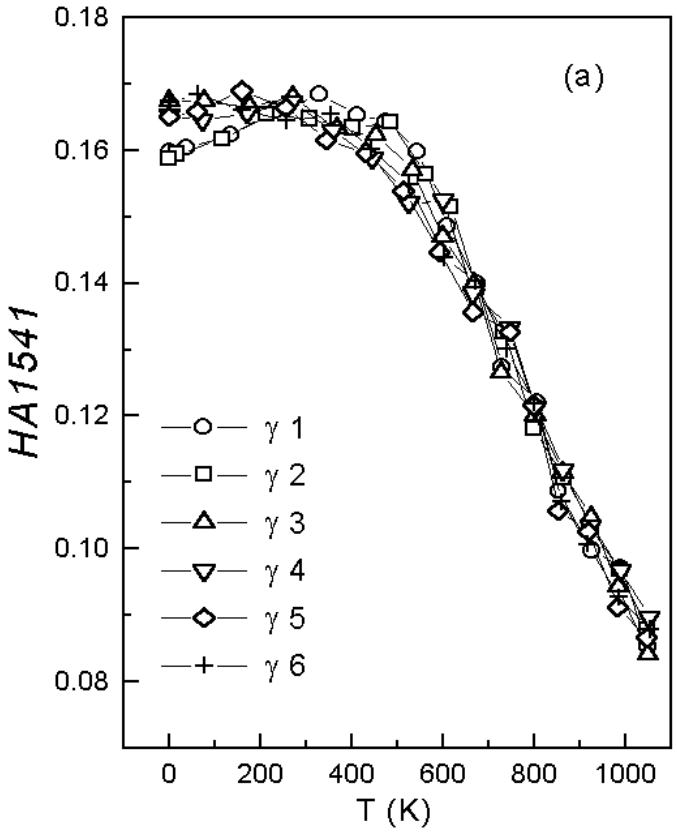

Figure 7. Relationship between relative number of 1541 pairs (*HA1541*) in (a) and 1431 pairs (*HA1431*) in (b) and temperature.

We further studied the possible transformation of 1551 pairs into 1541 pairs. First, we investigated the evolution of microstructure as the Al crystal was heated up and found that at about 600 K the 1541 pairs and 1431 pairs appear; with increasing temperature the 1541 and 1431 pairs increase and their ratio is two until the 1551 pairs appear. At about 800 K, the 1551 pairs appear and the ratio of 1541 pairs to 1431 pairs is smaller than two, while the ratio of the sum of the 1541 pair and 1551 pairs to the 1431 pairs is two. Second, using the recently developed activation–relaxation technique [28], we studied the relaxation and diffusion in amorphous Al. We observed the inter-transformation between 1541 pairs and 1551 pairs and the other transformations among various pairs. We also found that the probability of the transformation from 1551 pairs to 1541 pairs is larger than that from 1541 pairs to 1551 pairs. This is reasonable since most activation mechanisms lead to states of higher energy. The details of the transformation among various pairs will be presented elsewhere. Furthermore, the result in [29] shows that the ratio of the sum of 1541 and 1551 pairs to the 1431 pairs is 1.9 for amorphous Ni at 100 K, which is approximately equal to two the ratio of 1541 pairs to 1431 pairs in the interstitialcy model, and agrees with our results.

In [7] Jund *et al* have studied the fraction f_5 of pentagonal faces and the standard deviation σ_v of the cell-volume distribution (a large value of f_5 is a sign of strong icosahedral local order characteristic of a glass phase and σ_v describes the local density fluctuations). They have found that in the glass phase, with increasing quenching rates σ_v increases while f_5 remains constant

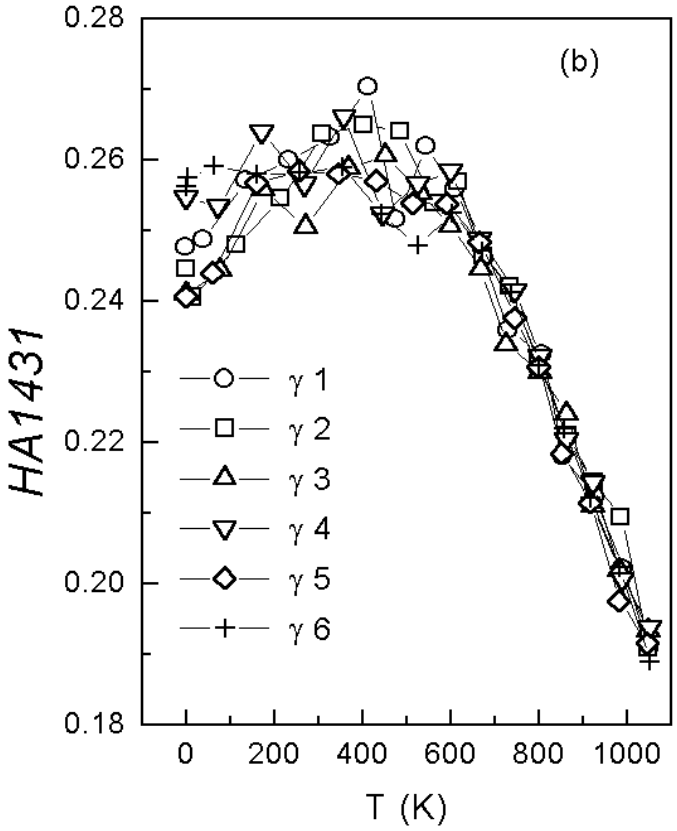

Figure 7. (Continued)

around 0.45, and the crystallization increases with increasing cooling rates. They concluded that the higher the local density fluctuations the higher the probability of finding crystal germs. Therefore, the faster the quenching rate the higher the probability of finding local arrangements close to crystal one, this leads to an increase in the crystallization with increasing cooling rates. Their results have also indicated that the glasses quenched at the critical rate separating glass forming and crystal forming have the highest structural stability. In that sense the critical rate can be view as an ideal rate. As they pointed out in their paper, they did not take into account the ability of the existent germs to grow and the microscopic origin of the existence of an ideal quenching rate remains to be elucidated. According to our present results, we may also obtain the same conclusion, that the glass stability increases with decreasing cooling rate, but we may have a completely different explanation. Here we may think the 1421 pairs as crystal germs, the 1541 and 1431 pairs may transform into the 1421 pairs based on the preceding discussion. The crystal germs grow by overcoming the resistance from the 1551 pairs, since crystal nucleation and icosahedral ordering are two competing tendencies. In particular, when the cluster of interpenetrating and face-sharing icosahedra percolates throughout the system as reported in [21], this resistance may be very strong. Our obtained results have shown that the faster the cooling rate the larger the 1551 pairs and the numbers of icosahedra (the same results are obtained by Kondo and Tsumuraya [25]). Therefore, the faster the cooling rate the smaller the resistance is, while the probability of finding crystal germs may be nearly the be same for

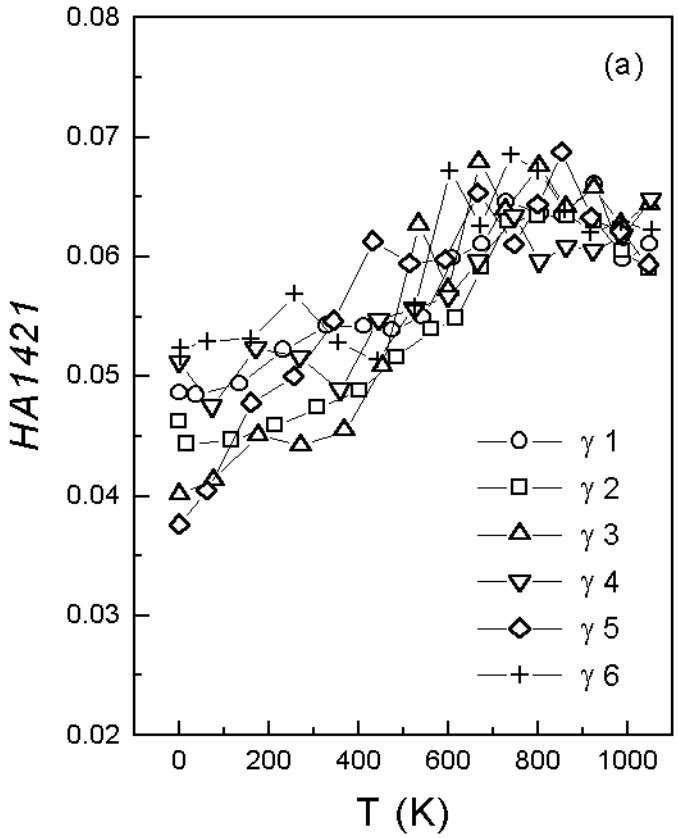

Figure 8. Relationship between relative number of 1421 pairs (*HA1421*) in (a) and 1422 pairs (*HA1422*) in (b) and temperature.

different cooling rates, or the dependence of this probability on the cooling rate is very weak. If p_+ stands for the probability of those pairs which increase with decreasing cooling rate, p_- for that of those pairs which decrease as the cooling rate decrease and p_c for that of those pairs which are nearly independent of the cooling rate, we may have an approximate equation: $p_+ + p_- = 1 - p_c$. A further decrease of the cooling rate leads to the further increase in the relative number of the 1551 pairs, the number of icosahedra and the perfection of defective icosahedra. Based on the above approximate equation and the *frustration* effect, the icosahedral ordering may have a saturation value which must already go beyond the *percolation threshold*. Thus, there exists a critical cooling rate, at which the icosahedra form a percolating cluster for the first time. Below the critical rate, there is a range of cooling rates at which the icosahedra can form a percolating cluster. The low limit of this range may be the ideal quenching rate in [7].

4. Conclusions

In summary, we have studied the dependence of the enthalpy, and the structural evolution of Al on cooling runs with the *glue* atomic potential. The changing trend of enthalpy with decreasing temperature is characteristic of the variation during the glass formation process. The enthalpy gives an observable but small dependence on the cooling rate. The strong dependence of

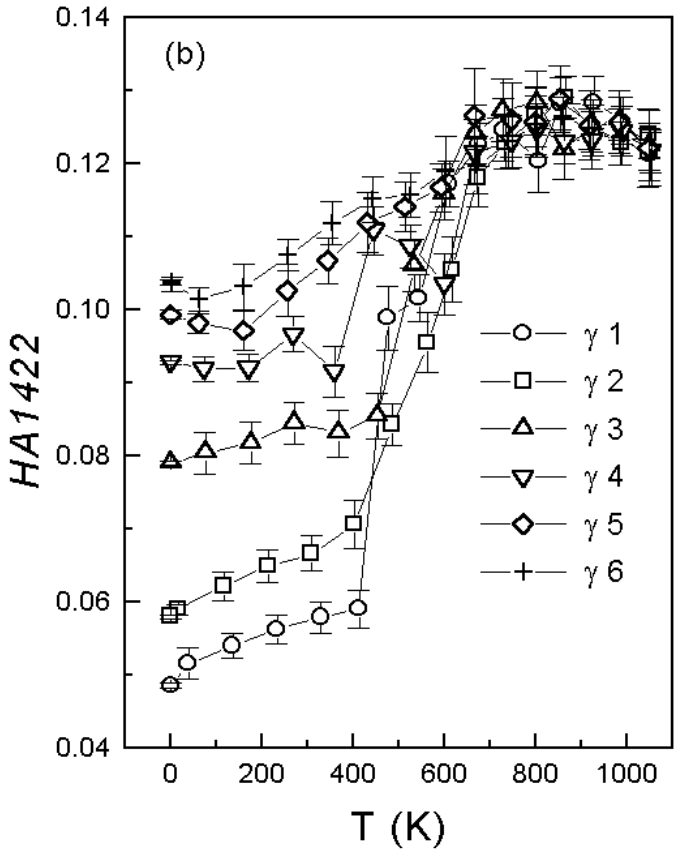

Figure 8. (Continued)

icosahedral ordering on the cooling rate is responsible for the dependence of the enthalpy on the cooling rate, while the almost independence of the 1541, 1431 and 1421 pairs of the cooling rate may result in that this dependence of the enthalpy on the cooling rate is small.

After glass transition, the 1541 and 1431 pairs hardly change with decreasing temperature and the structures of these two kinds of pair are similar to those in the fcc crystal containing interstitialcy. The results may be a good test on the interstitialcy model for condensed matter states of fcc metals. The faster the cooling rate is, the lower the probability of finding icosahedral ordering clusters is, so the smaller the resistance of the growth of the crystal germs is, while the probability of finding the crystal germs does not depend on the cooling rate. Our results also suggest that there exists a critical cooling rate below which the icosahedra form a percolating cluster and the glasses exhibit very strong stability. At a certain quenching rate, the strength of the icosahedral cluster network may have a saturation value or a maximum. This may be the origin for the existence of an ideal quenching rate at which the glass has the highest structural stability.

Acknowledgments

We are greatly indebted to Professor Q F Fang for his valuable discussions and J Y Tan and L J Zou for valuable help. C S Liu thanks N Mousseau for sending the code of the

activation–relaxation technique and useful discussion. This work was supported by the National Natural Science Foundation of China (grant No 19874067) and the Foundation of the Chinese Academy of Sciences (grant No KJ952-J1-412).

References

[1] Yang C Y, Sayers D E and Paesler M A 1987 *Phys. Rev.* B **36** 8122
Limbach C T and Gonser U 1988 *J. Non-Cryst. Solids* **106** 399
Johari G P, Hallbrucker A and Mayer E 1989 *J. Phys. Chem.* **93** 2648
[2] Brüning R and Samwer K 1992 *Phys. Rev.* B **46** 11 318
Brüning R and Sutton M 1994 *Phys. Rev.* B **49** 3124
[3] Fox J R and Andersen H C 1984 *J. Phys. Chem.* **88** 4019
Miyagawa H and Hiwatari Y 1989 *Phys. Rev.* A **40** 6007
Lai S K and Lin M S 1990 *J. Non-Cryst. Solids* **117/118** 907
[4] Vollmayr K, Kob W and Binder K 1995 *Europhys. Lett.* **32** 715
[5] Vollmayr K, Kob W and Binder K 1996 *J. Chem. Phys.* **105** 4714
[6] Vollmayr K, Kob W and Binder K 1996 *Phys. Rev.* B **54** 15 808
[7] Jund P, Caprion D and Jullien R 1997 *Phys. Rev. Lett.* **79** 91
[8] Daw M S and Bakes M I 1983 *Phys. Rev. Lett.* **50** 1285
Daw M S and Bakes M I 1984 *Phys. Rev.* B **29** 6443
[9] Finnis M W and Sinclair J E 1984 *Phil. Mag.* A **50** 45
[10] Ercolessi F, Parrinello M and Tosatti E 1984 *Phil. Mag.* A **58** 213
[11] Ercolessi F and Adams J B 1994 *Europhys. Lett.* **26** 583
[12] Chen K Y, Liu H B, Li X P, Han Q Y and Hu Z Q 1995 *J. Phys.: Condens. Matter* **7** 2379
[13] Lu J and Szpunar J A 1997 *Phil. Mag.* A **75** 1057
Wang L H, Liu H Z, Chen K Y and Hu Z Q 1997 *Physica* B **239** 267
[14] Sun D Y and Gong X G 1998 *Phys. Rev.* B **57** 4730
[15] Andersen H C 1980 *J. Chem. Phys.* **72** 2383
Brown D and Clarke J H R 1984 *Mol. Phys.* **51** 1243
[16] Lu K and Li Y 1998 *Phys. Rev. Lett.* **80** 4474
[17] Honecutt J D and Andersen H C 1987 *J. Phys. Chem.* **91** 4950
[18] Frank F C 1952 *Proc. R. Soc.* A **215** 43
Nelson D R and Toner J 1981 *Phys. Rev.* B **24** 363
[19] Steinhardt P J, Nelson D R and Ronchett M 1981 *Phys. Rev.* B **28** 784
[20] Abraham F F 1980 *J. Chem. Phys.* **72** 359
[21] Jonsson H and Andersen H C 1988 *Phys. Rev. Lett.* **60** 2295
[22] Baschnagel J, Binder K and Wittmann H-P 1993 *J. Phys.: Condens. Matter* **5** 1597
[23] Liu R S, Qi D W and Wang S 1992 *Phys. Rev.* B **45** 451
Liu R S and Wang S 1992 *Phys. Rev.* B **45** 451
Liu C F and Wang S 1992 *J. Phys.: Condens. Matter* **4** 6729
[24] Qi D W and Wang S 1991 *Phys. Rev.* B **44** 884
[25] Kondo T and Tsumuraya K 1991 *J. Chem. Phys.* **94** 8220
[26] Granato A V 1992 *Phys. Rev. Lett.* **68** 974
[27] Nordlund K and Averback R S 1998 *Phys. Rev. Lett.* **80** 4201
[28] Barkema G T and Mousseau N 1996 *Phys. Rev. Lett.* **77** 4358
Mousseau N and Barkema G T 1997 *Phys. Rev.* E **57** 2419
Barkema G T and Mousseau N 1998 *Phys. Rev. Lett.* **81** 1865
[29] Posada-Amarillas A and Garzón I L 1996 *Phys. Rev.* B **53** 8363